ECS Transactions, 35 (5) 117-122 (2011)
10.1149/1.3570785 ©The Electrochemical Society

Subband Structure Engineering in Silicon-on-Insulator FinFETs using Confinement

Z. Stanojevic, V. Sverdlov, and S. Selberherr

Institute for Microelectronics
TU Wien, Gußhausstraße 27-29, 1040 Wien, Austria

Splitting between equivalent valleys larger than the spin splitting energy is observed in confined electron systems, e.g. Si films grown either on SiGe substrate or Si dioxide and Si/SiGe quantum dots. Understanding the contribution of different factors in the valley degeneracy lifting is of key importance for the development of spin-based devices in Si. We demonstrate that the splitting between equivalent valleys strongly depends on the confinement direction and that it is orientation dependent. To explain the effect we use a simple but accurate two-band **k·p** model for the conduction band in silicon. Our data is in good agreement with recent results obtained by first-principle calculations.

Introduction

The gradual approach of MOSFET miniaturization to saturation puts limitations on the continuation of the performance increase in logic circuits, and a search for alternative computational principles and technologies becomes necessary. The quantum computer is using quantum mechanical properties to reproduce the structure of data in its operation, which promises a substantial computational superiority over a classical computer for certain problems. The fundamental unit of quantum information is the qubit, while in a conventional computer the information is stored binary. The principle of quantum computation is based on quantum mechanical superposition and entanglement of quantum states. Qubits can be constructed from quantum states of atomic ions, quantum dots, superconducting Josephson junctions, or carrier spins.

Silicon, the material most widely used by the semiconductor industry, possesses several properties attractive for spin-based applications: weak spin-orbit interaction and predominantly zero spin nuclei. Because of these properties electron spin states in silicon should show increased stability which results in a long lifetime of spin polarized carriers. Recently (1), a possibility to inject spin polarized current into silicon was demonstrated. A coherent propagation of spin current through a silicon wafer of 350μm thickness was achieved.

The conduction band of silicon consists of six equivalent valleys. In (100) quantum wells and inversion layers the valley degeneracy is partly lifted. However, the quantum numbers of the two remaining degenerate values compete with those of the electron spin potentially threatening the stability of the qubit. In order to build a silicon based spin qubit it is necessary to lift the remaining valley degeneracies sufficiently so that the corresponding two-level system is only formed by the spin degree of freedom. In order to prevent valley degrees of freedom from interfering with spin quantum numbers, it is mandatory to develop a method for controlling the valley splitting.

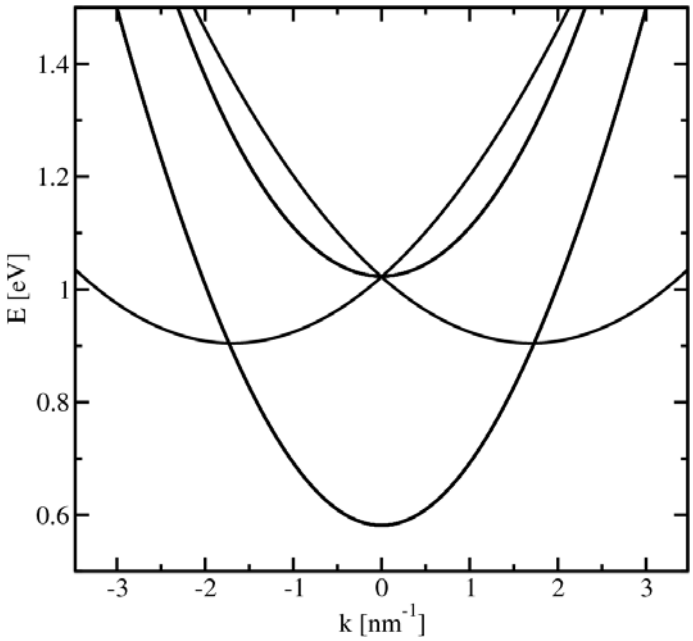

Figure 1. Subband structure in a [100] 2nm thick circular fin. The unprimed subbands are four-times degenerate. Primed subbands are centered at k_0.

The ability to build structures with atomistic precision is one of the goals of the rapidly developing nanotechnology. The control over the wave function or the spin of a single dopant is a key element in silicon quantum electronics. Recent progress in dopant engineering, coherent control over dopant states, and robust operation provides an accelerating momentum to the development of silicon quantum electronic devices. However, due to valley degeneracy, exchange coupling between two dopants in silicon is extremely sensitive to the inter-donor position (2). Controllable valley splitting opens a possibility to tune the coupling between the dopants thus relaxing the requirement for their relative displacement to be unreasonably small.

Valley splitting was discovered in the mid sixties and has been the subject of intensive investigation ever since. Recently, the theory of intervalley coupling was extended (3) to explain experimental data (4). Intervalley coupling was introduced phenomenologically at the heterostructure interfaces. The strength of the intervalley interaction parameter was then calculated by calibrating results to a tight-binding model. Estimations show that the valley splitting is in the range of 0.5meV, which is in agreement with experiments on laterally confined electron systems in point contacts. However, a much smaller valley splitting was reported in Si/SiGe heterostructures (4). In order to make the theoretical predictions qualitatively consistent with the experimental data, a quantum well slightly misaligned from (001) orientation has been considered in (3). The misalignment results in (001) atomic steps at the interface. This makes the valley splitting inhomogeneous and position-dependent. It was suggested in (3) that only the areas with high valley splitting contribute to the experimental signal. Regardless of numerous efforts, the contribution of different factors including interface disorder and quantization remains one of the greatest theoretical challenges on the path of understanding valley splitting. Recently, an experimental observation of valley splitting in Si/SiGe quantum dots was reported in (5) and an explanation of the large valley splitting at the Si/SiO_2 interface observed in (6) by hybridization of the valley states with

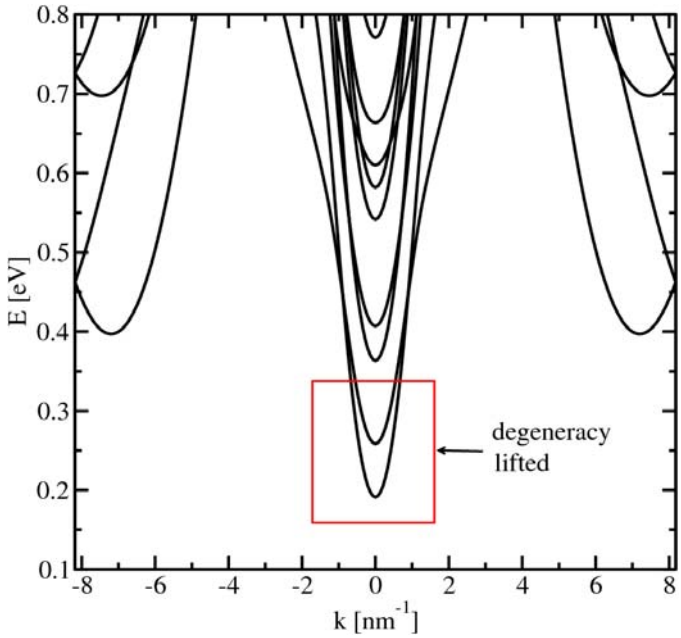

Figure 2. Subband structure in a [110] oriented 2nm thick circular fin. The two-fold degeneracy of the unprimed subbands is completely removed.

the interface states (7) was given. Control over valley splitting is one of the ingredients necessary for the successful implementation of Si spin devices.

In this work, we demonstrate the enhancement of the valley splitting in silicon fin structures and nanowires along the [110] direction. Multi-gate FinFETs are a promising alternative to bulk MOSFETs beyond the 22nm technology node.

Method

The subband structure in a confined system is computed using the **k·p** model proposed in (8), which has been shown to be accurate up to 0.5eV above the conduction band edge (9). For two valleys along [001] direction the Hamiltonian is

$$H = \begin{pmatrix} \frac{p_z^2}{2m_l} + \frac{p_x^2 + p_y^2}{2m_t} + \frac{p_z \hbar k_0}{m_l} + U(\mathbf{r}) & \frac{p_x p_y}{M} \\ \frac{p_x p_y}{M} & \frac{p_z^2}{2m_l} + \frac{p_x^2 + p_y^2}{2m_t} - \frac{p_z \hbar k_0}{m_l} + U(\mathbf{r}) \end{pmatrix}, \qquad [1]$$

where $\mathbf{p} = -i\hbar\,\mathrm{d}/\mathrm{d}\mathbf{r}$ is the momentum operator, $U(\mathbf{r})$ is the confinement potential, m_t and m_l are the transversal and the longitudinal effective masses, $k_0 = 0.15 \times 2\pi / a$ is the position of the valley minima relative to the X point in unstrained silicon, and $M^{-1} \approx m_t^{-1} - m_0^{-1}$. The Hamiltonians for the valleys along [100] and [010] can be obtained from [1] by appropriate coordinate transformation. The resulting Schrödinger differential equation with the Hamiltonian [1] is discretized using the box integration method and solved for each value of the conserved momentum along the directions of the wave function propagation using efficient numerical algorithms available through the Vienna Schrödinger-Poisson framework (VSP).

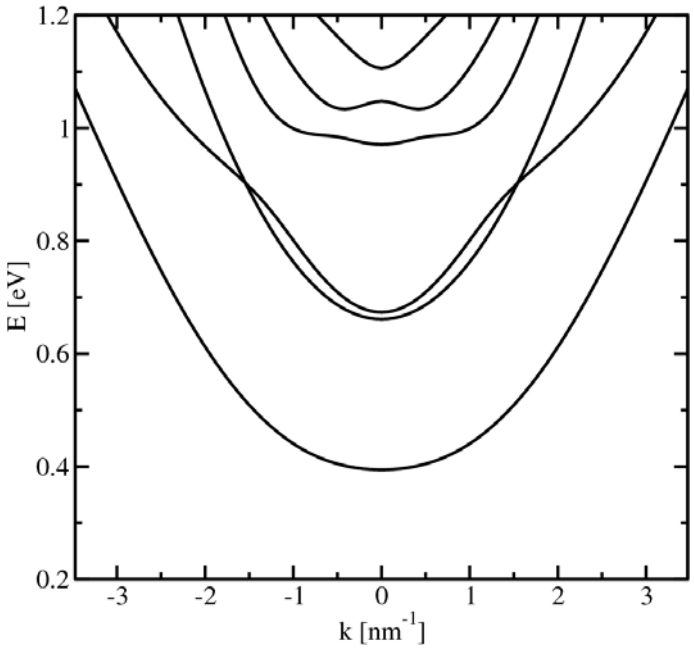

Figure 3. Subband structure in a [111] 2nm thick circular fin. The lowest subband is six-fold degenerate. Its minimum is located at the Γ-point.

Results

Fins and nanowires of [100], [110], and [111] growth orientation of circular, square, and rectangular cross sections have been investigated. The subband structure for a circular 2nm thick nanowire is shown in Fig.1-Fig.3. The circular shape of nanowires is most closely related to the shapes studied previously in (10) using a tight-binding (TB) method. The electron subband dispersion computed with the **k·p** model possesses all the important features obtained with an atomistic-based calculations, regardless its approximate character as compared to TB.

In the case of the [100] nanowire confinement causes the minima of the unprimed subbands to be projected onto the Γ-point of the one-dimensional Brillouin zone, while the minima of the primed subbands are located at $\pm k_0$ (see Fig.1). The unprimed subbands of the [100] nanowire are four-fold degenerate within the **k·p** model. In the [110] nanowire the degeneracy of the lowest subband is completely lifted as seen in Fig.2, and the lowest subband becomes non-degenerate. For the 2nm thick [111] nanowire the lowest subband minim is at the Γ-point (Fig.3), which is in agreement with TB calculations (10). The lowest subband preserves six-fold degeneracy. The degeneracy can be partly lifted in a square structure with the faces along (11-2) and (1-10) directions. Yet, the lowest subband remains four-fold degenerate.

We now turn our attention to the case of the [110] oriented nanowire shown in Fig.2. It is worth noticing that in the effective mass approximation the lowest subband must be two-fold degenerate because of the equivalency between the two valleys oriented along the [001] direction. Surprisingly, within the more accurate **k·p** model the degeneracy is removed. Similar results were obtained from the TB approach (10). The degeneracy of the lowest subband is completely lifted for a square or rectangular [110] nanowire, with the faces oriented along (001) and (-110) directions. Fig.4 demonstrates that the degeneracy is lifted in both circular and square [110] fins. Furthermore, the degeneracy is lifted for the higher unprimed subband as well. For thin fins the splitting between the

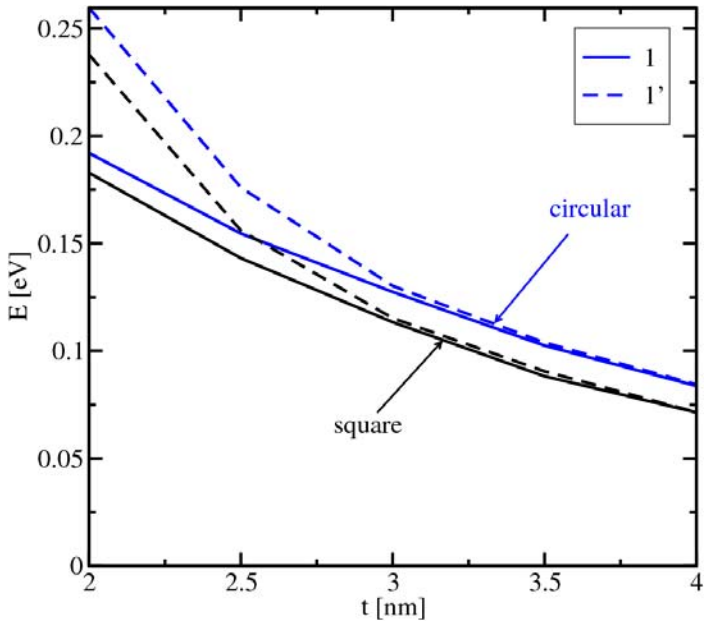

Figure 4. Dependence of the minima of the two lowest subbands on the fin thickness in circular and square [110] fins. The two-fold degeneracy is lifted in thin fins.

subbands originating from the two equivalent [001] valleys, i.e. the valley splitting, can be large. Fig.5 demonstrates good agreement between the valley splitting obtained from the **k·p** model and results of recent density functional calculations (11). For thin [110] fins valley splitting may reach a value of about one electron-volt. Thus, one can control and engineer the valley splitting between the equivalent valleys by properly designing the shape and size of silicon fins.

In order to explain such a large valley splitting let us approximate the fin confinement potential by a square well with infinite potential walls. The subband minimum is at the Γ-

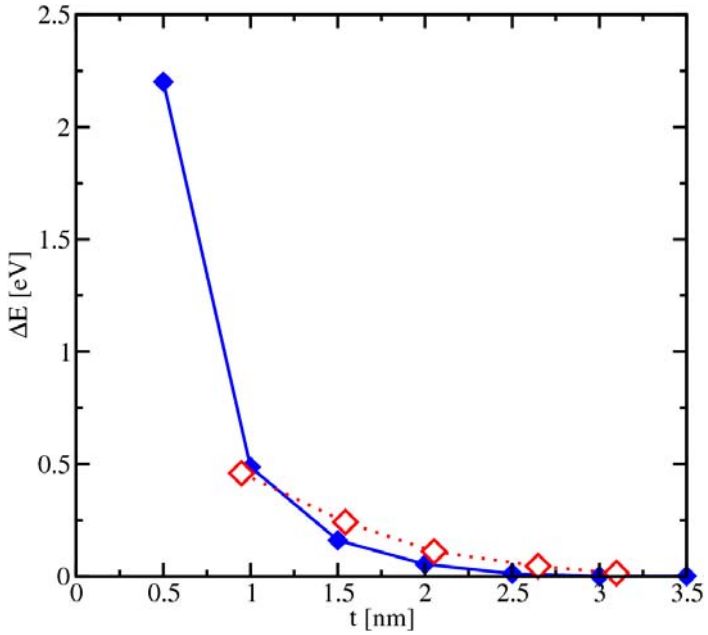

Figure 5. Comparison between the valley splitting dependences on the square fin thickness obtained with the **k·p** model [1] (filled symbols) and from density functional calculations (11).

point. At this point the off-diagonal term in the Hamiltonian [1] in a [110] fin is equal to $[\pi n\hbar/(2tM)]^2$, where n is an integer and t is the fin thickness. The non-zero value of the off-diagonal elements results in a non-parabolic dispersion along [001] direction for [001] valleys. For the quantization along the [001] direction a consideration similar to the one in ultra-thin body silicon films can be applied (9). If the value of the off-diagonal elements is not too large, the valley splitting is given by (9)

$$\Delta E_{m,n} = \left(\frac{\pi}{k_0 t}\right)^4 \frac{\hbar^2 k_0^2 m^2 n^2}{2Mk_0 t\,|1-(\pi m/k_0 t)^2|}\sin(k_o t)\,, \qquad [2]$$

where m is another integer corresponding to the quantization along the [001] axis. The relative valley splitting of the first subband $E_{1,1} = \frac{\pi^2\hbar^2}{2m_l t^2}\left(1+\frac{m_l}{m_t}\right)$ is

$$\frac{\Delta E_{1,1}}{E_{1,1}} = \left(\frac{\pi}{k_0 t}\right)^2 \frac{m_l}{Mk_0 t\,|1-(\pi m/k_0 t)^2|\,(1+m_t/m_l)}\sin(k_o t)\,, \qquad [3]$$

which varies strongly with the fin thickness.

Conclusion

A rigorous analysis of the subband structure in silicon fins of different shape and orientation has been performed. It is demonstrated that within the two-band **k·p** model the two-fold degeneracy of unprimed subbands with the same quantum number is completely lifted in [110] oriented fins. The relative splitting between the unprimed subbands is inversely proportional to the third power of the fin thickness and becomes large rapidly, when the fin thickness is decreased. The valley splitting can be reliably controlled by designing the shape and orientation of a silicon fin, which is of a great importance for developing silicon spin-based devices.

Acknowledgments

This work is supported by the European Research Council through the grant #247056 MOSILSPIN.

References

1. B.Huang, D.Monsma, I.Appelbaum, *Phys. Rev. Lett.* **99**, 177209 (2007).
2. S.Das Sarma, R.de Sousa, X.Hu, B.Koiller, *Solid-State Commun.*, **133**, 737 (2005).
3. M.Friessen, S.Chutia, C.Tahan,S.N.Coppersmith, *Phys.Rev.B* **75**, 115318 (2007).
4. S.Goswami, K.A.Slinker, M.Friesen, L.M.McGuire, J.L.Truitt, C.Tahan, L.J.Klein, J.O.Chu, P.M.Mooney, D.W.van der Weide, R.Joynt, S.N.Coppersmith, M.A.Eriksson, *Nature Physics* **3**, 41 (2007).
5. M.Borselli, R.Ross, A.Kiselev, E.Croke, K.Holabird, P.Deelman, L.Warren, I.Alvarado-Rodriguez, I.Milosavljevic, F.Ku, W.Wong, A.Schmitz, M.Sokolich, M.Gyure, A.Hunter., arXiv:1012.1363.
6. K.Takashina, Y.Ono, A.Fujiwara, Y.Takahashi, Y.Hirayama, *Phys.Rev.Lett.* **96**, 236801 (2006).
7. A.L.Saraiva, B.Koiller, M.Friesen, *Phys.Rev.B* **82**, 245314 (2010).
8. J.C.Hensel, H.Hasegawa, M.Nakayama, *Phys.Rev*. **138**, A225 (1965).
9. V.Sverdlov, O.Baumgartner, T.Windbacher, S.Selberherr, *J.Computational Electron.*, **8**, 192 (2009).
10. A.Svizhenko, P.W.Leu, K.Cho, *Phys.Rev.B* **75**, 125417 (2007).
11. H.Tsuchiya, H.Ando, S.Sawamoto, T.Maegawa, T.Hara, H.Yao, M.Ogawa, *IEEE T-ED* **57**, 406 (2010).